Bulletin of Environment, Pharmacology and Life Sciences
Bull. Env.Pharmacol. Life Sci., Vol 11[2] January 2022 : 129-136

Online ISSN 2277-1808
Journal's URL:http://www.bepls.com
CODEN: BEPLAD

ORIGINAL ARTICLE **OPEN ACCESS**

Fabrication of g-C_3N_4 nanosheets reinforced with Myricetin Functionalized AgNPs for its potential bactericidal effect

Noushad Karuvantevida[a,b], Gnanasekar Sathishkumar[a,d], Rabah Iratni[c], Sivaperumal Sivaramakrishnan[a*]

[a]Department of Biotechnology, Bharathidsasan University, Tiruchirappalli 620024, Tamilnadu, India
[b]College of Medicine, Mohammed Bin Rashid University of Medicine and Health Sciences, Dubai, United Arab Emirates.
[c]Department of Biology, College of Science, United Arab Emirates University, Al-Ain, P.O. Box 15551, United Arab Emirates.
[d]School of Materials and Energy, Southwest University, Chongqing, P.R. China 400715

ABSTRACT

Developing new drugs and technology to combat multi drug-resistant microorganisms (MDR) bacteria is crucial. Furthermore, biofunctionalization of nanocomposites confer safe features and value for prospective nanomedicine applications. Henceforth, the goal of this study was to synthesize polymer-coated g-C_3N_4 that was then decorated with a metal-flavonoid nanocomplex structure using in situ hybridization. The synthesized nanocomposite, CS@g-C_3N_4/MY-AgNPs has uniform surface distribution, which was characterized by X-ray diffraction, FT-IR spectra, SAED, FE-SEM, and HR-TEM. According to FTIR result of nanocomposite (NC), the ligand hydroxyl groups of Myricetin (MYR) interact with the soft metal ions during nanoparticle (NP) formation. XRD and SAED pattern revealed the existence of polycrystalline material. Moreover, the results of FE-SEM and HR-TEM analysis showed the crystallite size of 21±11 nm. The strong signals for C, N, and Ag obtained by EDAX analysis indicate that Ag NPs are strongly immobilised on the g-C_3N_4 surface. In addition, The result of the bactericidal activity of the CS@g-C_3N_4/MY-AgNPs outperformed the negative control, with inhibition zones of 12±0.5, 16±0.69, 16±0.28, 16±0.32, 15±1, 13±1, 16±0.25, 15±0.28, and 17±0.5 mm against K. pneumoniae, E. coli, V. cholera, P. vulgaris, S. dysenteriae, MRSA, Streptococcus pneumoniae, P. aeruginosa, and Bacillus sp., respectively. The study's findings can be used for a variety of biological applications in the near future.

Keywords: *biofunctionalization; nanocomposites; Myricetin; X-ray Diffraction; bacterial pathogens*

Received 01 .01.2022 Revised 19.01.2022 Accepted 25.01.2022

INTRODUCTION

Bacterial infections remains as major challenge in healthcare sector for many decades, inflicting significant deformities and mortality each year [3]. Since the 1930s, a variety of antibiotic medications derived from natural entities have been found, mostly to prevent the growth of bacterial infections [11]. However, the persistence and emergence of multi drug resistance (MDR) or super bugs has evolved into a worldwide epidemic, owing mostly to inadequate sanitation, a lack of quick diagnosis, and antibiotic misuse [17]. On the other hand, the normal cleaning using chemical disinfectants is expensive, time-consuming, and does not provide long-term protection against bacterial pathogen recolonization. As a result, it is critical to create new medications and technologies to tackle MDR microorganisms [2]. Unprecedented efforts and investments have been made to develop the most reliable therapeutic options [4].

Several advanced functional materials have been developed in the past decade to obtain improved bactericidal efficiency with minimal nonspecific effects. Noble metal nanoparticles (MNPs) such as silver (Ag), gold (Au), copper (Cu), platinum (Pt), and palladium (Pd) were considered possible nanosystems for various biomedical applications among the diverse nanomaterials. Silver nanoparticles (Ag NPs) have a high bactericidal activity compared to other MNPs, and they are being studied extensively in the antibacterial study. Their low stability due to oxidation, accumulation, and poor biocompatibility, on the other hand, is a downside for applications. Ag NPs are mixed with other noble metal nanoparticles, metal oxides, and biopolymers, and in some instances, they are transformed into core-shell nanostructures to resolve this downside [11]. MNPs are given a good boost by 2D nanomaterials, which allows for fine dispersion and stability. Two-dimensional (2D) nanomaterials, For example, Graphitic-phase carbon

nitride (g-C_3N_4) nanosheets, a soft and conjugated polymer, are well-known for their ability to act as affinity support for the conjugation of other compounds. Due to their specific properties, such as good biocompatibility, low cost, fast preparation, and low toxicity. The g-C_3N_4-based materials have been explored for various biomedical applications such as antibacterial, phototherapy, biosensor, imaging, and diagnostic applications. Several recent studies have shown that g-C_3N_4 may be a viable candidate for bactericidal photocatalysts [8, 9]. However, the antibacterial efficiency of g-C_3N_4 relies on their physio-chemical, optical and electronic properties. It has been reported that the nanocomposites of g-C_3N_4 possess enhanced antibacterial effect for wide range bio applications [22].

Many natural products have recently been discovered to have promising antibiotic and antiviral effects. In particular, flavonoids are a class of natural organic compounds and secondary metabolites with a wide range of biological functions, pharmacological effects, and antiviral properties [Kesarkar et al., 2009]. Among them, Myricetin (MYR) is a dietary flavonoid with various biological properties, including antibacterial, antioxidant, and anticancer functions [Williamson *et al*., 2018]. A variety of drug-delivery technologies are being tested to address bioavailability problems. As a result, this study aimed to establish a green chemistry method for exfoliating g-C_3N_4 and hybridized with MYR-capped AgNPs for antibacterial applications.

MATERIAL AND METHODS

Materials

Melamine(MW, 126.12), Myricetin (MW, 318.24), and Chitosan were purchased from Sigma Aldrich, USA. Silver nitrate and all other chemicals were procured from Himedia, Mumbai, India.

Synthesis of bulk-g-C_3N_4

Bulk g-C_3N_4 was synthesized through melamine thermal polycondensation, as previously described in the literature [22]. Prior to synthesis, melamine was ground into powder in an agate mortar for 30 minutes. The melamine was then placed in an alumina crucible with a lid, and pure nitrogen (99.999 %) was added before being heated to 550 °C in a muffle furnace at a rate of 20 °C per minute for 120 minutes. After the stock had cooled to room temperature, it was removed and grounded into a fine light yellow powder with the mortar.

Exfoliation of CS@g-C_3N_4

To exfoliate g-C_3N_4 nanosheets, 80 mg of bulk g-C_3N_4 was ultrasonically combined in 60 ml of distilled water for 10 h. After sonication, 40 ml of 1% acetic acid solution containing chitosan (40 mg) was added and well mixed for 1 h with a stirrer. The hybrid solution was then ultrasonicated for another 6 h. Following sonication, the CS@g-C_3N_4 composite was separated by centrifugation at 12000 rpm for 10 minutes. The final pellet was collected and freeze-dried to obtain CS@g-C_3N_4 composite powder for further studies.

Fabrication of CS@g-C_3N_4/MYR-AgNPs

For the synthesis of MYR-AgNPs decorated CS@g-C_3N_4, 30 mg of CS@g-C_3N_4 was combined with 60 ml of water and sonicated for 1 h for fine dispersion for *in situ* synthesis and hybridization of AgNPs (Solution A). Simultaneously, 10 mL of 5 mM $AgNO_3$ were prepared and mixed with 30 mL of 50% ethanol containing 2mM MYR (Solution B). Then, the solution B was injected drop-wise into Solution A (pH-9) while constantly stirring and maintaining the pH-9 using 10M NaOH. After 3 h, the end-product was collected by a centrifugation step at 12000 rpm for 10 minutes at 4° C and purified thrice using distilled water. The pellet was freeze-dried and the powder was kept at 4° C for future research.

Characterization of CS@g-C_3N_4/MYR-AgNPs

The surface chemistry of synthesized CS@g-C_3N_4/MYR-AgNPs was investigated using FTIR spectroscopic measurements. After mixing the samples with KBr powder and drying them, the transmittance was measured using a Shimadzu spectrometer (Wavelength range between 4000 cm^{-1} to 400 cm^{-1}). Moreover, X-ray diffraction (XRD) analysis was performed to determine the dimension of synthesized CS@g-C_3N_4/MYR-AgNPs with h, k, l values. The most popular and versatile method for determining the size distribution and stability of CS@g-C_3N_4/MYR-AgNPs in liquids was determined using Dynamic Light Scattering (DLS). FE-SEM analysis was used to evaluate the morphology of the synthesized CS@g-C_3N_4/MYR-AgNPs. In which, 25 L of diluted material was sputter-coated on a copper stub for electron microscopic examinations, and micrographs of CS@g-C_3N_4/MYR-AgNPs were recorded using HITACHI SU6600 FE-SEM operating at 15.0 keV. Then, HR-TEM analysis was carried out to investigate the fine morphology of CS@g-C_3N_4/MYR-AgNPs wherein the metal nanoparticles were dried on a carbon-coated copper grid before being examined with a JEOL JEM 2100 HR-TEM equipped with an EDAX attachment.

In vitro antibacterial studies

Bacterial cultures

Bacterial pathogens such as *Klebsiella pneumoniae* **(MTCC 530),** *Escherichia coli* (*MTCC***1687)**, *Vibrio cholera* (*MTCC***0139)**, *Pseudomonas* (*MTCC***512**), *Proteus vulgaris* (*MTCC* 426), *Shigella dysenteriae* (*ATCC* **13313),** *Streptococcus aureus* **(MTCC 121),** *Methicillin-resistant* ***Staphylococcus aureus***(MRSA-clinical isolate obtained from a hospital), *Streptococcus pneumoniae* (*MTCC* 7465*), Bacillus sp.* (*MTCC***511)** were collected from the Microbial Type Culture and Collection (MTCC) in Chandigarh, India.

Well-Diffusion assay

Agar well diffusion experiment had been used to investigate the preliminary antibacterial activity of synthesized CS@g-C_3N_4/MYR-AgNPs. All of the bacterial pathogens were grown in Mueller-Hinton medium at 37 °C before being subcultured in Mueller-Hinton agar overnight. The bacterial colonies were then suspended in 2 mL of sterile saline, and the test pathogen inoculum was generated by diluting the sterile saline to adjust the turbidity of the bacterial suspensions to 0.5 McFarland (1.5×10^8 colony forming units CFU/mL).

RESULTS AND DISCUSSION

Fabrication of CS@g-C_3N_4/MY-AgNPs

In general, natural polymers have been studied for their possible application in engineering of materials for various biomedical applications. The bulk g-C_3N_4 produced from the hydrothermal conversion of melamine forms a non-homogenous dispersion in aqueous medium. As demonstrated in Scheme 1, the natural polymer, chitosan acts as a good exfoliating agent in the ultrasonication process to fabricate g-C_3N_4 nanosheets. Upon the addition of MY-$AgNO_3$ solution into CS@g-C_3N_4 (pH-9), the reaction mixture becomes dark brown, which clearly suggest the formation/deposition of MY-AgNPs on CS@g-C_3N_4 surface. Following CS modification, the color of g-C_3N_4 was changed to white, and subsequently to black after MY-AgNPs decoration (Prabakaran & Pillay, 2021). Liu et al., 2016 also reported a similar phenomenon in which the addition of grape seed extract to a combination of $AgNO_3$ and C_3N_4 changes the color from yellow to brownish-yellow at different concentrations, suggesting that the size of AgNPs increases with concentration. In another investigation, actinomycetes extract was combined with $AgNO_3$ without the inclusion of any 2D material to synthesize AgNPs (Vimala et al., 2022b).

Characterization of CS@g-C_3N_4/MY-AgNPs

XRD patterns of as-synthesized CS@g-C_3N_4/MY-AgNPs shows a weaker peak at 27.26° (JCPDS, 87–1526) corresponding to the (002) plane of exfoliated CS@g-C_3N_4. Other notable peaks at 38.1, 43.4, 64.4, and 77.4 were assigned to the (111), (200), (220), and (311) planes of the face-centered cubic (fcc) crystalline Ag^0 (JCPDS, 65–2871). Furthermore, it was clearly noticed that the crystal structure of g-C_3N_4 remains intact even after MY-AgNPs deposition. The existence of highly distributed Ag species in the composites was attributed to the increased intensities of Ag planes. Meanwhile, it was reported that the diffraction intensities peak at 27.5 was weakened upon increasing Ag concentration increases, as the diffraction peak of Ag species grow. These findings suggest that the MY-AgNPs were successfully deposited on the surface of g-C_3N_4 (Ren et al., 2021).

The FE-SEM micrographs of as-prepared CS@g-C_3N_4/MY-AgNPs displays the significant number of AgNPs decoration on CS@g-C_3N_4 sheets. Furthermore, the micrographs validating that the MY-AgNPs are evenly distributed across the sheets with minimal aggregation. A similar phenomenon have been reported earlier, in which the prepared g-C_3N_4 nanosheets were several micrometres size confirming the effective exfoliation of BCN. Further, the HR-TEM analysis was used to observe the fine structures of AgNPs on the g-C_3N_4 surface, as shown in Figure 5a. Approximately the size of around 50 particles were measured using image J software, and the mean diameter was 21±11 nm. The SAED pattern revealed the existence of polycrystalline material with intense patches of (111), (200), (220), and (311) of Ag crystals' fcc lattice (Figure 5b). EDAX-analysis generated the strong signals for C, N, and Ag (Figure 5c), indicating the strong immobilization of Ag NPs on the g-C_3N_4 surface.

Moreover, the FTIR spectra of CS@g-C_3N_4 and as-prepared CS@g-C_3N_4/MYR-AgNPs were shown in Figure 3a and b. The CS@g-C_3N_4 shows absorption peak at 3434.92 cm^{-1}, 2358.94 cm^{-1}, 1635.64 cm^{-1}, and 655.80. Also, the as-prepared CS@g-C_3N_4/MYR-AgNPs generate very similar transmittance with slight variations. A wideband at 3332.99 cm^{-1} is due to the strong stretching vibrations of the O–H functional group of MYR, and 2358.94 cm^{-1} manifests the existence of aliphatic groups of CS. The strong 1633.17 cm^{-1} was due to the vibration of the carbonyl (C=O) functional group. The similarity of AgNPs decorated g-C_3N_4 with MYR also indicates the successful re-combination of the functional group on MYR with as-prepared Ag/g-C_3N_4 nanocomposite, improving the stability of the nanocomposite. This data, as predicted, clearly shows that MYR's hydroxyl groups were involved in redox reaction with Ag ions and forms AgNPs. The distinctive absorption band of carbonyl group moved in the MY-AgNPs spectra. It confirms that the hydroxyl groups of MYR were oxidized to carbonyl groups during metal ion reduction via hydrogen bonding interaction. Following that, the electrons of carbonyl group would transfer the free orbit of metal ions during

reduction process, resulting in the fabrication of AgNPs. As a result, the MYR would act as capping/stabilizing agent on the metal NPs. Our results suggest that the hard ligand hydroxyl groups of MYR interact with the soft metal ions during NPs formation [14, 7].

***In vitro* antibacterial studies**

Antimicrobial activity of synthesized NMs and NCs against human pathogens such as *K. pneumoniae* (MTCC 530), *E. coli* (*MTCC* 1687), *V. cholera* (*MTCC* 0139), *Pseudomonas* (*MTCC* 512), *P. vulgaris* (*MTCC* 426), *S. dysenteriae* **(***ATCC 13313*), *S. aureus* (MTCC 121), *MRSA* (clinical isolate obtained from a hospital), *Streptococcus pneumoniae* (*MTCC* 7465***)***, *Bacillus sp.* (*MTCC* 511) were tested (Figure 6). When compared to NMs, the antibacterial activity of NCs was shown to be more effective against both gram-negative and gram-positive bacterial strains. NCs had inhibition zones of 12±0.5, 16±0.69, 16±0.28, 16±0.32, 15±1, 13±1, 16±0.25, 15±0.28, and 17±0.5 mm against *K. pneumoniae, E. coli, V. cholera, P. vulgaris, S. dysenteriae, MRSA, Streptococcus pneumoniae, P. aeruginosa, and Bacillus sp.,* respectively (Table 1). Myricetin did not show antibacterial activity except *P. aeruginosa.* The negative control lacked antibacterial action against the microorganisms [15]. The overall result showed that the synthesized CS@g-C_3N_4 and CS@g-C_3N_4/MY-AgNPs outperformed the negative control in terms of bactericidal activity. Gram +ve bacteria displayed stronger bactericidal activity than Gram –ve bacteria, which is most likely due to cell surface charge and contact according to the data. Two methods have been postulated to explain the activity of Ag@g-C_3N_4. (1) Ag@g-C_3N_4 NSs can produce highly reactive oxygen species (ROS) capable of oxidizing biofilm nucleic acids, proteins, and polysaccharides. (2) Furthermore, AgNPs can bind to DNA, cell membranes, and cellular proteins, causing cell death [6].

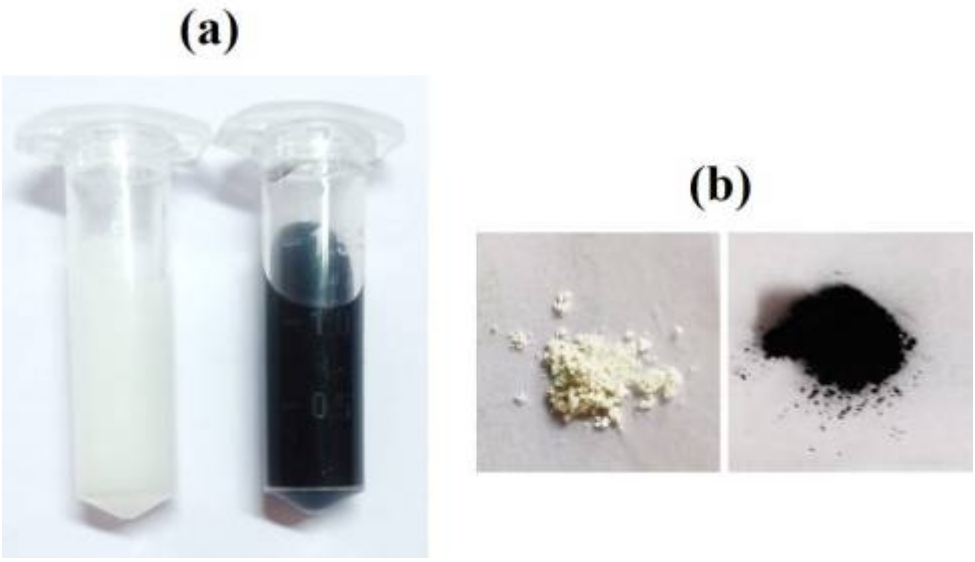

Figure 1. Exfoliation of g-C_3N_4 and fabrication of CS@g-C_3N_4/MYR-AgNPs (a) Colour variation from white to dark brown clearly indicates the *in situ* hybridization process (b) Powder samples of pure CS@g-C_3N_4 (white) and CS@g-C_3N_4/MYR-AgNPs (black).

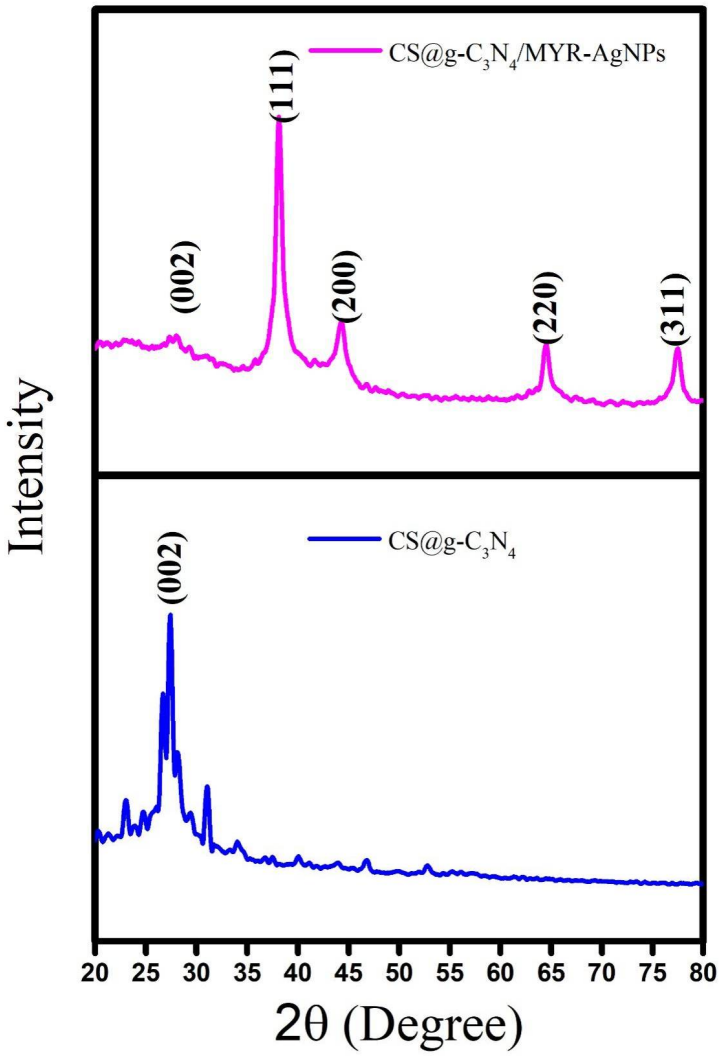

Figure 2. XRD analysis of CS@g-C_3N_4/MYR-AgNPs

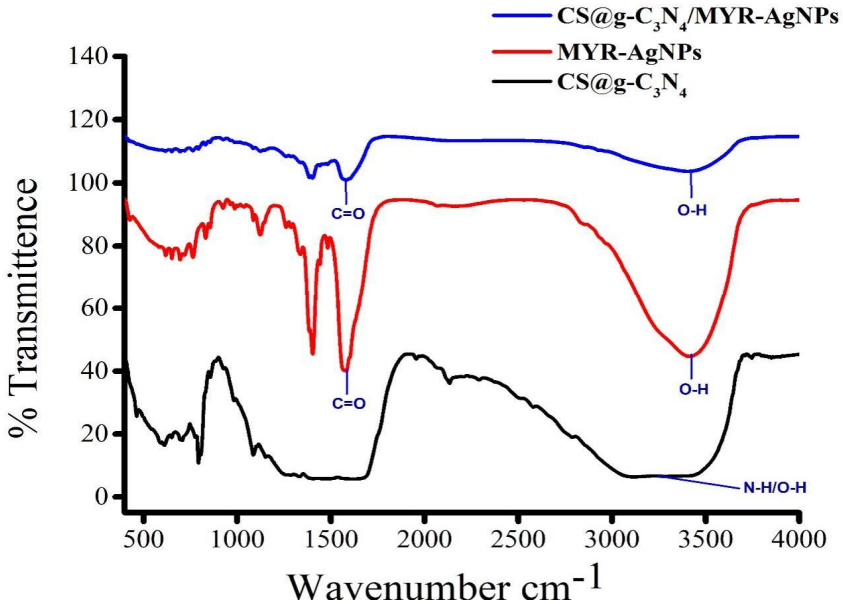

Figure 3. FT-IR analysis of (a) CS@g-C_3N_4 and (b) as-prepared CS@g-C_3N_4/MYR-AgNPs

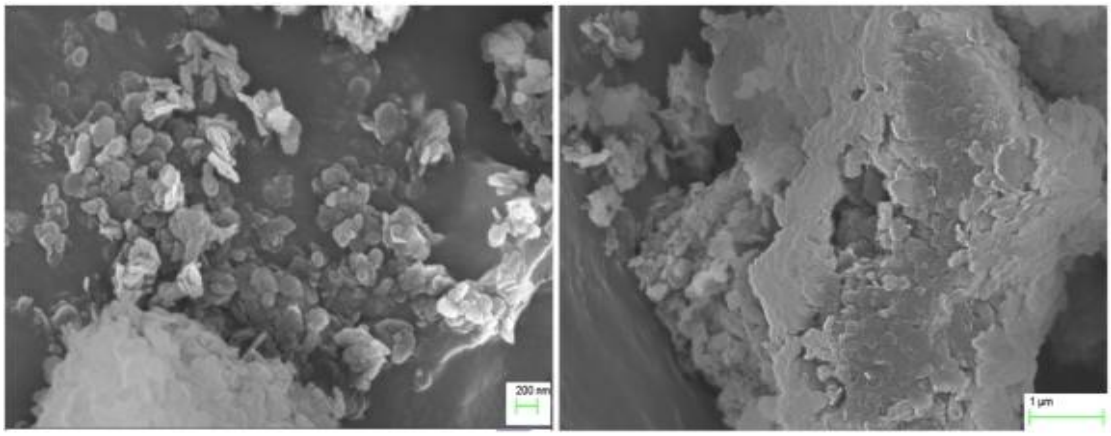

Figure 4. FE-SEM micrographs of CS@g-C_3N_4/MYR-AgNPs

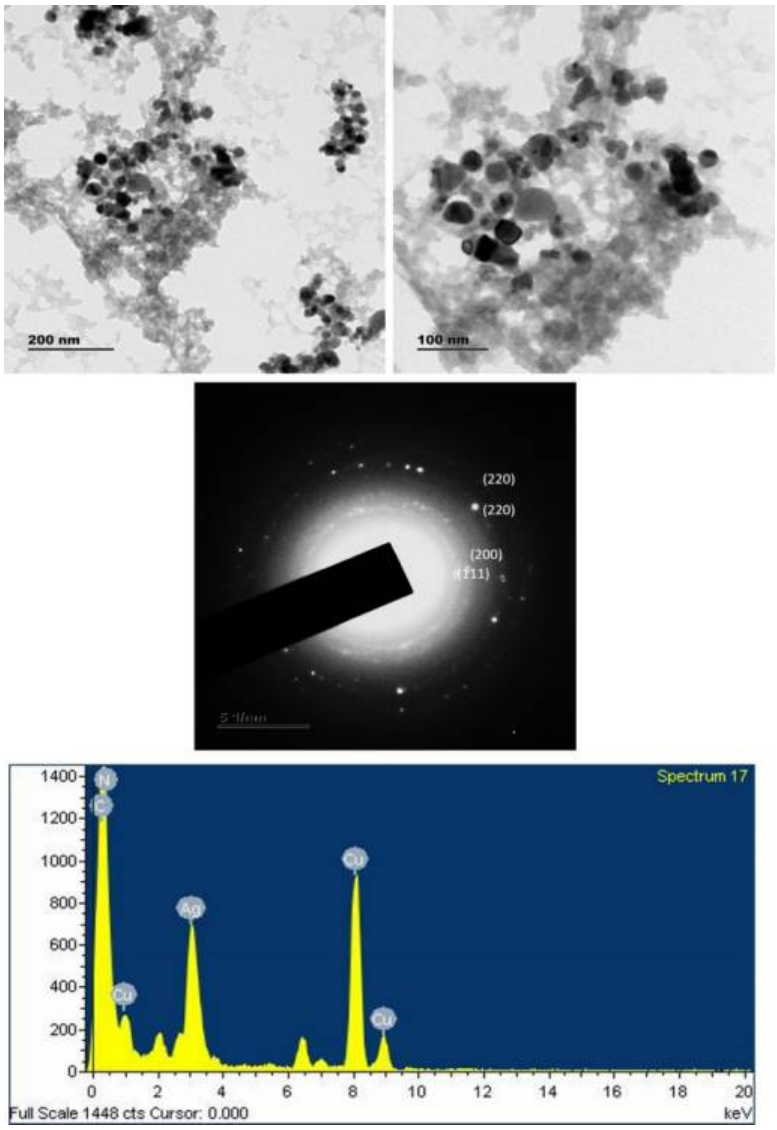

Figure 5. HR-TEM analysis (a) HR-TEM micrographs (b) SAED pattern and (c) EDAX analysis of CS@g-C_3N_4/MYR-AgNPs

Figure 6. *In vitro* antibacterial activity of CS@g-C_3N_4/MYR-AgNPs by well-diffusion method
A- Negative control; B- MYR; C- CS@g-C_3N_4/MYR-AgNPs; D-CS@C_3N_4; E- Positive control (Streptomycin)

Table 1 *In vitro* antibacterial activity of CS@g-C_3N_4/MYR-AgNPs by well-diffusion method
A- Negative control; B- MYR; C- CS@g-C_3N_4/MYR-AgNPs; D-CS@C_3N_4; E- Positive control (Streptomycin)

S. No.	PATHOGEN	A (mm±Std)	B (mm±Std)	C (mm±Std)	D (mm±Std)	E (mm±Std)
1.	*K. pneumoniae*	6±0	6±0.1	12±0.5	6±0	23±1
2.	*S. dysenteriae*	6±0	6±0	15±1	6±0	25±0.1
3.	*E. coli*	6±0	6±0.1	16±0.69	6±0	21±0.5
4.	*Pseudomonas*	6±0	11±0	15±0.28	6±0.1	26±1
5.	*P. vulgaris*	6±0	6±0.1	16±0.32	6±0.5	24±0.1
6.	*Bacillus sp.*	6±0	6±0.15	17±0.5	6±0.2	25±0.5
7.	*V. cholera*	6±0	6±0.1	16±0.28	6±0.5	24±1
8.	*S. pneumoniae*	6±0	6±0	16±0.25	6±1	24±0.5
9.	*MRSA*	6±0	6±0.1	13±1	6±0.5	24±0.5
10	*S.aureus*	6±0	6±0.1	14±0.76	6±0.1	26±0.5

CONCLUSION

A simple green chemistry-based liquid-phase exfoliation process was designed to synthesize polymer-coated g-C_3N_4, which was then decorated with a metal-flavonoid nanocomplex structure by *in situ hybridization*. Based on these results, we can conclude that, hybrid nanocomposites had a higher yield with a smaller size, a quicker synthesis rate, and excellent antibacterial action against both gram-negative and gram-positive bacteria. As a consequence, the findings of this study indicate to a novel technique for producing AgNPs and g-C_3N_4-based hybrid nanocomposites with varying surface functionalities that may be exploited in a variety of biological applications in the future.

NOTES

The authors declare no competing financial interest.

ACKNOWLEDGEMENTS

The authors acknowledge and thank the RUSA 2.0, biological science (Rashtriya Uchchatar Shiksha Abhiyan 2.0), Bharathidasan University, Trichy for providing financial support during this research work.

REFERENCES

1. Dadigala, R., Bandi, R., Gangapuram, B.R. and Guttena, V., (2017). Carbon dots and Ag nanoparticles decorated g-C_3N_4 nanosheets for enhanced organic pollutants degradation under sunlight irradiation. *Journal of Photochemistry and Photobiology A: Chemistry*, 342, pp.42-52.
2. De Kraker, M.E., Stewardson, A.J. and Harbarth, S., (2016). Will 10 million people die a year due to antimicrobial resistance by 2050?. *PLoS medicine*, *13*(11), p.e1002184.
3. Dhingra, S., Rahman, N.A.A., Peile, E., Rahman, M., Sartelli, M., Hassali, M.A., Islam, T., Islam, S., Haque, M. (2020). Microbial resistance movements: an overview of global public health threats posed by antimicrobial resistance, and how best to counter. *Frontiers in Public Health*, 8, 531.

4. Gnanasekar, S., Balakrishnan, D., Seetharaman, P., Arivalagan, P., Chandrasekaran, R. and Sivaperumal, S., (2020). Chrysin-anchored silver and gold nanoparticle-reduced graphene oxide composites for breast cancer therapy. *ACS Applied Nano Materials*, 3(5), pp.4574-4585.
5. Gnanasekar, S., Palanisamy, P., Jha, P.K., Murugaraj, J., Kandasamy, M., Mohamed Hussain, A.M.K. and Sivaperumal, S., (2018). Natural Honeycomb Flavone Chrysin (5, 7-dihydroxyflavone)-Reduced Graphene Oxide Nanosheets Fabrication for Improved Bactericidal and Skin Regeneration. *ACS Sustainable Chemistry & Engineering,* 6(1), pp.349-363.
6. Khan, M.E., Han, T.H., Khan, M.M., Karim, M.R. and Cho, M.H., (2018). Environmentally sustainable fabrication of Ag@ g-C_3N_4 nanostructures and their multifunctional efficacy as antibacterial agents and photocatalysts. *ACS Applied Nano Materials*, *1*(6), pp.2912-2922.
7. Li, Z., Ma, W., Ali, I., Zhao, H., Wang, D., Qiu, J. (2020). Green and Facile Synthesis and Antioxidant and Antibacterial Evaluation of Dietary Myricetin-Mediated Silver Nanoparticles. *ACS omega*, 5(50), 32632-32640.
8. Liu, C., Wang, L., Xu, H., Wang, S., Gao, S., Ji, X., Xu, Q. and Lan, W., (2016). "One pot" green synthesis and the antibacterial activity of g-C3N4/Ag nanocomposites. *Materials Letters*, 164, pp.567-570.
9. Liu, R., Chen, Z., Yao, Y., Li, Y., Cheema, W.A., Wang, D. and Zhu, S., (2020). Recent advancements in g-C_3N_4-based photocatalysts for photocatalytic CO_2 reduction: a mini review. *RSC Advances*, *10*(49), pp.29408-29418.
10. Murugan, E., Santhoshkumar, S., Govindaraju, S. and Palanichamy, M., (2021). Silver nanoparticles decorated g-C_3N_4: An efficient SERS substrate for monitoring catalytic reduction and selective Hg^{2+} ions detection. Spectrochimica Acta Part A: *Molecular and Biomolecular Spectroscopy*, 246, p.119036.
11. Peterson, E., Kaur, P. (2018). Antibiotic resistance mechanisms in bacteria: relationships between resistance determinants of antibiotic producers, environmental bacteria, and clinical pathogens. *Frontiers in microbiology*, 2928.
12. Prabakaran, E., Pillay, K. (2021). Self-Assembled Silver Nanoparticles Decorated on Exfoliated Graphitic Carbon Nitride/Carbon Sphere Nanocomposites as a Novel Catalyst for Catalytic Reduction of Cr (VI) to Cr (III) from Wastewater and Reuse for Photocatalytic Applications. *ACS omega*, 6(51), 35221-35243.
13. Ren, T., Dang, Y., Xiao, Y., Hu, Q., Deng, D., Chen, J. and He, P., (2021). Depositing Ag nanoparticles on g-C3N4 by facile silver mirror reaction for enhanced photocatalytic hydrogen production. *Inorganic Chemistry Communications*, 123, 108367.
14. Sathishkumar, P., Li, Z., Huang, B., Guo, X., Zhan, Q., Wang, C. and Gu, F.L., (2019). Understanding the surface functionalization of myricetin-mediated gold nanoparticles: Experimental and theoretical approaches. *Applied Surface Science*, 493,634-644.
15. She, P., Li, J., Bao, H., Xu, X. and Hong, Z., (2019). Green synthesis of Ag nanoparticles decorated phosphorus doped g-C_3N_4 with enhanced visible-light-driven bactericidal activity. *Journal of Photochemistry and Photobiology A: Chemistry*, *384*, p.112028.
16. Urnukhsaikhan, E., Bold, B.-E., Gunbileg, A., Sukhbaatar, N., Mishig-Ochir, T. (2021). Antibacterial activity and characteristics of silver nanoparticles biosynthesized from *Carduus crispus.Scientific Reports,* 11(1), 1-12.
17. Ventola, C.L., (2015). The antibiotic resistance crisis: part 1: causes and threats. *Pharmacy and therapeutics*, *40*(4), p.277.
18. Vimala, R., Rajivgandhi, G., Sridharan, S., Jayapriya, M., Ramachandran, G., Kanisha, C.C., Manoharan, N., Li, W.-J. (2022a). Antimicrobial Activity of Extracellular Green-Synthesized Nanoparticles by Actinobacteria. in: Methods in Actinobacteriology, *Springer*, 717-720.
19. Vimala, R., Rajivgandhi, G., Sridharan, S., Jayapriya, M., Ramachandran, G., Kanisha, C.C., Manoharan, N., Li, W.-J. (2022b). Biosynthesis and Characterization of Silver Nanoparticles from Actinobacteria. in: Methods in Actinobacteriology, *Springer,* 709-712.
20. Williamson, G., Kay, C.D. and Crozier, A., (2018). The bioavailability, transport, and bioactivity of dietary flavonoids: A review from a historical perspective. *Comprehensive Reviews in Food Science and Food Safety*, *17*(5), pp.1054-1112.
21. Yan, K., Mu, C., Meng, L., Fei, Z., Dyson, P.J. (2021). Recent advances in graphite carbon nitride-based nanocomposites: structure, antibacterial properties and synergies. *Nanoscale Advances*, 3(13), 3708-3729.
22. Yan, S.C., Li, Z.S. and Zou, Z.G., 2009. Photodegradation performance of g-C_3N_4 fabricated by directly heating melamine. *Langmuir*, 25(17), pp.10397-10401.

CITATION OF THIS ARTICLE

N Karuvantevida, G Sathishkumar, R Iratni, S Sivaramakrishnan. Fabrication of g-C_3N_4 nanosheets reinforced with Myricetin Functionalized AgNPs for its potential bactericidal effect**.** Bull. Env.Pharmacol. Life Sci., Vol 11[2] January 2022 : 129-136